INSTITUTE OF PHYSICS PUBLISHING SUPERCONDUCTOR SCIENCE AND TECHNOLOGY

Supercond. Sci. Technol. **19** (2006) S540–S544 doi:10.1088/0953-2048/19/7/S23

Heat propagation analysis in HTSC bulks during pulse field magnetization

Hiroyuki Fujishiro[1], Shusuke Kawaguchi[1], Masahiko Kaneyama[1], Atsushi Fujiwara[1], Tatsuya Tateiwa[1] and Tetsuo Oka[2]

[1] Faculty of Engineering, Iwate University, 4-3-5 Ueda, Morioka 020-8551, Japan
[2] IMRA Material R&D Co. Limited, 5-50 Hachiken-cho, Kariya 448-0021, Japan

E-mail: fujishiro@iwate-u.ac.jp

Received 16 December 2005, in final form 14 February 2006
Published 2 May 2006
Online at stacks.iop.org/SUST/19/S540

Abstract

The time evolutions of the three-dimensional temperature profiles in a superconducting bulk disc have been calculated after applying a pulse field in the pulse field magnetization (PFM) by use of a finite element method (FEM). The total generated heat Q, experimentally estimated using the maximum temperature rise ΔT_{max} and specific heat C of the bulk, used in the analysis and the distribution of Q in the periphery region of the bulk, is suitably supposed in order that the calculated time evolutions of temperatures $T(t)$ reproduce the measured ones on the bulk surface. From the analysis, the heat generation during PFM takes place under adiabatic conditions because the total Q value is about one or two orders of magnitude larger than the cooling power of the cryocooler used. The enhancement of the total heat capacity by setting a stainless steel ring onto the bulk as a heat reservoir is one of the effective methods to reduce the temperature rise and to enhance the trapped field.

1. Introduction

For the practical applications of high-T_c superconducting (HTSC) bulks as a strong bulk magnet system, pulse field magnetization (PFM) has been intensively developed, as well as conventional field cooled magnetization (FCM). In the PFM process, however, a large amount of the heat generation occurs due to the dynamical motion of the magnetic fluxes relative to the FCM process, resultantly reducing the trapped field B_T^P at temperatures below 77 K [1]. We have measured the time dependences of the temperature $T(t)$ on the bulk surface during PFM at several positions and have systematically investigated the relation between B_T^P and $T(t)$ [2–4]. We have recently developed a new PFM method using the modified multi-pulse technique with stepwise cooling (MMPSC), and attained B_T^P as high as 5.20 T on the surface of a GdBaCuO bulk superconductor 45 mm in diameter, which originates from the precise investigation of the temperatures on the bulk [5]. $B_T^P = 5.20$ T is currently the highest value using PFM. In this way, monitoring the temperature is a valuable tool in understanding the field trapping phenomena during PFM. The temperature rise is, however, generally inhomogeneous in the bulk due to the inhomogeneous distribution of the critical current density J_c and the existence of growth sector boundaries (GSBs). Since the number of measuring positions in the temperature and trapped field must be finite in an actual experimental setup, it is desirable to numerically obtain the three-dimensional profile of temperature $T(t, \vec{x})$ in the bulk in order to precisely understand the field trapping mechanism in PFM. The heat propagation analysis combined with the electro-magnetic phenomena using a finite element method (FEM) is a powerful tool in analysing the PFM procedure [6]. However, it is difficult for the numerical analysis to take account of the inhomogeneous distribution of J_c in an actual bulk.

In this paper, we apply the FEM analysis only to the heat propagation in the bulk during PFM. The time evolution and spatial distribution of the three-dimensional temperatures $T'(t, \vec{x})$ have been calculated to reproduce the measured temperatures $T(t, \vec{x})$ on the bulk surface. We discuss the heat propagation phenomena in the bulk cooled by the helium refrigerator after applying the pulse field and suggest the desired direction in PFM to enhance the trapped field B_T^P.

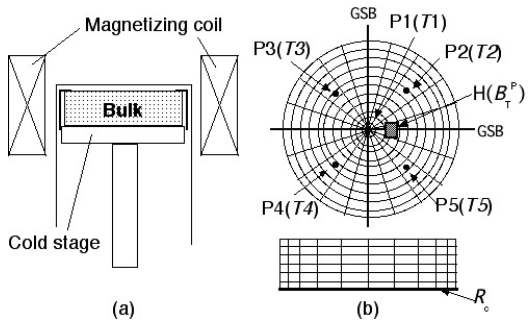

Figure 1. (a) Experimental setup around the bulk and the magnetizing coil. (b) The positions of the temperature ($T1$–$T5$) and the trapped field (B_T^P) measurements on the bulk surface are indicated. The bulk disc is equally divided into the elements for the numerical analysis (see text).

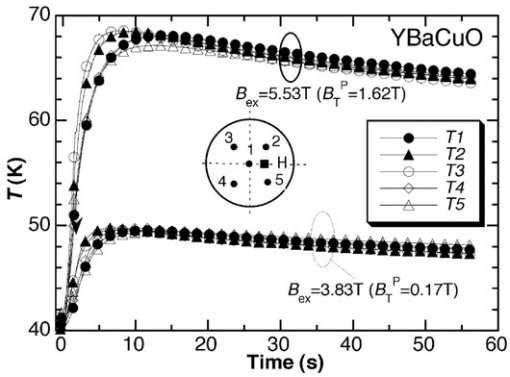

Figure 2. The time evolutions of temperatures $T(t)$ for respective positions on the YBaCuO bulk after applying a pulse field of $B_{ex} = 3.83$ and 5.53 T at $T_s = 40$ K.

2. Experimental details

Highly c-axis oriented YBaCuO and SmBaCuO bulks (Dowa Mining Co, Ltd, 45 mm in diameter and 15 mm in thickness) were used for the measurements and the analyses. The experimental setup around the bulk disc is presented in figure 1(a). The bulk was stacked on the cold stage of the Gifford McMahon (GM) cycle helium refrigerator using an indium foil and was cooled down and fixed at $T_s = 40$ K in a vacuum chamber. Five sets of fine chromel–constantan thermocouples were adhered at the bulk centre (P1) and each growth sector region (GSR) (P2–P5, 12 mm distant from P1). The time dependences of temperature ($T1(t)$–$T5(t)$) were measured about seven times per second after applying the magnetic pulse. The bulk was magnetized using a solenoid-type pulse coil dipped in liquid N_2, where pulse fields of $B_{ex} = 3.83$ and 5.53 T were applied with the rise time of 12 ms. The trapped field B_T^P was measured using a Hall sensor (Bell, model BHA 921) adhered on the centre of the bulk surface (position H).

The heat propagation analysis was performed by solving a three-dimensional heat diffusion equation using a commercial code (PHOTO-THERMO^{TM} by PHOTON Ltd, Japan). For the numerical analysis, the bulk disc was equally divided into 20 elements along the circumferential direction, 10 elements along the radial direction and 6 elements along the thickness direction, respectively, as shown in figure 1(b). The upper and side surfaces of the bulk were supposed to be adiabatic and the cold stage to be a constant temperature ($T_s = 40$ K) as boundary conditions. The thermal contact resistance R_c between the lower bulk surface and the cold stage was considered as a fitting parameter for the calculation. In the analysis, the magnitude and the spatial distribution of the generated heat after applying a magnetic pulse must be decided in order to reproduce the observed $T(t, \vec{x})$ at each position on the bulk surface. The total generated heat Q was estimated using the maximum temperature rise ΔT_{max} and the specific heat C of the bulk [7]. $C(T)$ for each bulk was calculated using the relation $C = \kappa/\alpha$, i.e., the thermal conductivity κ divided by the thermal diffusivity α, both of which were measured simultaneously [8]. Since the magnetic fluxes always intrude into the bulk from the periphery region during PFM, the heat generation should be the largest at the periphery, and it decreases on approaching the bulk centre. For simplicity in the analysis, we suppose that the heat generation occurs only in the outermost periphery element layer. The time evolutions of the three-dimensional temperature $T'(t, \vec{x})$ were calculated to minimize the residual differences between the measured and calculated temperatures for each bulk and for various applied fields B_{ex}. In the calculation, the ab-plane and c-axis thermal conductivities κ_{ab}, κ_c and the density d of each bulk were referred to in the database [9].

3. Results and discussion

3.1. Determination of thermal contact resistance R_c

Figure 2 presents the time evolutions of temperatures $T(t)$ for respective positions on the YBaCuO bulk after applying a pulse field of $B_{ex} = 3.83$ and 5.53 T [2]. For each B_{ex}, the nearly homogeneous temperature changes occur at $T1$–$T5$ with a small difference in the rise time. These results suggest that the pinning force F_p is nearly identical in each GSR and that the magnetic fluxes homogeneously intrude into the bulk from the periphery. The temperature rise for $B_{ex} = 5.53$ T is larger than that for $B_{ex} = 3.83$ T. The Q value estimated using the ΔT_{max} for $T2$ is 160 J and 450 J, and the trapped field B_T^P at position H is 0.17 T and 1.62 T for $B_{ex} = 3.83$ and 5.53 T, respectively.

Figure 3 shows the calculated temperature $T2'(t)$ on the YBaCuO bulk for several boundary conditions after applying a pulse field of $B_{ex} = 3.83$ T. In this analysis, we supposed that $Q = 160$ J was equally divided by 20 and each heat element was arranged in the outermost surface layer, taking account of the results shown in figure 2. In the ideal boundary condition with $R_c = 0$, the calculated $T2'(t)$ shows a clear peak at $t = 1$ s, suddenly decreases and then returns to the initial temperature for $t = 20$ s. This result does not reproduce the measured $T2(t)$. The $T2'(t)$ profile depends on the R_c value and can fairly reproduce the measured one, when the R_c value is supposed to be 5000 times the thermal resistance of the bulk along the c-axis ($=5000/\kappa_c$). The heat generation after applying a pulse field is terminated within the pulse duration ($\sim$0.1 s) [10] and the Q value is about one or two orders of magnitude larger than the cooling power of the GM cycle helium refrigerator used, which is as small as 1 W ($=1$ J s^{-1})

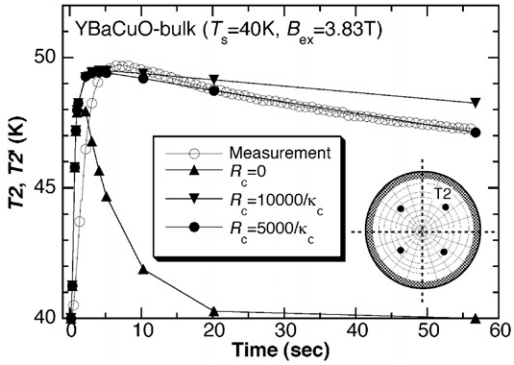

Figure 3. The calculated temperature $T2'(t)$ on the YBaCuO bulk for several thermal contact resistances R_c after applying a field of $B_{ex} = 3.83$ T at $T_s = 40$ K.

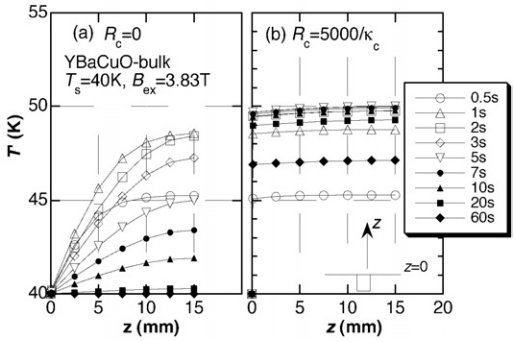

Figure 4. The calculated temperature profile along the thickness direction (z-direction) as a function of time t for (a) $R_c = 0$ and (b) $R_c = 5000/\kappa_c$.

at 40 K. These results suggest that the heat generation during PFM in the bulk must take place under adiabatic conditions. As a result, the R_c value determined by the analysis mainly comes from the excess heat generation, which cannot be absorbed by the cooling power. In the subsequent analysis, we use the R_c value ($=5000/\kappa_c$) as a thermal contact resistance between the lower bulk surface and the cold stage.

3.2. Spatial dependence of temperature change in YBaCuO bulk

Figure 4 shows the calculated temperature profile $T'(t, z)$ in the YBaCuO bulk along the thickness direction (z-direction) as a function of time t in the case of (a) $R_c = 0$ and (b) $R_c = 5000/\kappa_c$ after applying a pulse field $B_{ex} = 3.83$ T. In this figure, the position $z = 15$ mm coincides with the position P2 on the bulk surface. For $R_c = 0$, which is an unrealistic condition, the temperature $T'(t, 0)$ at the lower bulk surface ($z = 0$) is fixed at 40 K and is independent of t. The calculated temperature $T'(t, z)$ in the bulk increases after applying a pulse field, has a maximum at $t = 1$ s and then decreases. On the other hand, for the actual situation with $R_c = 5000/\kappa_c$ shown in figure 4(b), $T'(t, z)$ rises up uniformly and sharply in the whole bulk due to the adiabatic character, has a maximum at $t = 5$ s and then decreases at $t = 60$ s. It is found that a temperature gradient hardly exists along the z-direction.

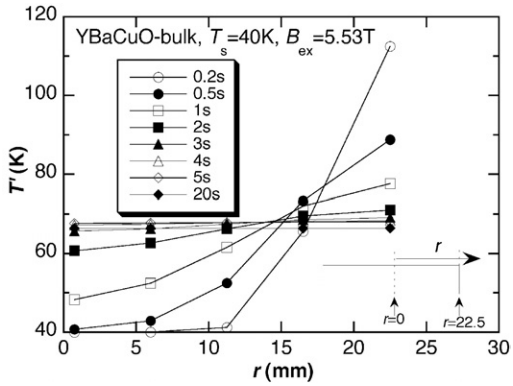

Figure 5. The calculated temperature profiles $T'(t)$ on the bulk surface along the radius direction (r-direction) after applying a pulse field of $B_{ex} = 5.53$ T to the YBaCuO bulk.

Figure 5 presents the time evolution of the calculated temperature profile $T'(t, r)$ on the surface of the YBaCuO bulk along the radius direction (r-direction) through the bulk centre and the position P2, after applying a higher pulse field of $B_{ex} = 5.53$ T. It should be noticed that the calculated temperature $T'(t, r)$ at the edge of the bulk ($r = 22.5$ mm) reaches 113 K at $t = 0.2$ s, which is far higher than the superconducting transition temperature T_c (=90 K). $T'(t, r)$ at the edge quickly decreases to 78 K at $t = 1$ s and then gradually decreases. $T'(t, r)$ at the centre ($r = 0$) increases relatively more slowly than that at the outer surface and then decreases. These results at P1 ($r = 0$ mm) and P2 ($r = 12$ mm) reproduce the experimental ones shown in figure 3 well.

3.3. Inhomogeneous heat generation in SmBaCuO bulk

Figure 6(a) indicates the experimental results of temperature changes $T(t)$ of the SmBaCuO bulk after applying a pulse field of $B_{ex} = 3.83$ T [3]. $T4$ and $T5$ sharply rise up with a clear peak but $T2$ and $T3$ increase moderately, in contrast to the YBaCuO bulk shown in figure 2(a). These results suggest that the magnetic fluxes preferably intrude into the bulk from these two positions (P4 and P5) due to the weaker pinning force F_p. The trapped field B_T^P was as small as 0.24 T at position H because the B_{ex} value to magnetize the bulk sufficiently was fairly small. Figure 6(b) indicates the calculated temperature profiles $T'(t)$ at each position. In this case, the generated heat Q was 240 J, which was estimated using the average of the maximum temperature rises at P2–P5. The distribution of the heat generation was decided most suitably at the most outer surface as shown in the inset of figure 6(b). The calculated $T'(t)$ can reproduce the measured $T(t)$ at each position.

Figure 7 shows the measured $T(t)$ and the calculated $T'(t)$ for the SmBaCuO bulk after applying a pulse field of $B_{ex} = 5.53$ T [3]. In figure 7(a), all the maximum temperatures T_{max} increase compared with those for $B_{ex} = 3.83$ T shown in figure 6(a) and the spatial dependences of $T(t)$ in four GSRs become small. These results suggest that the heat-generating region expands due to the large amount of flux intrusions. For the $T'(t)$ calculation, the estimated Q value of 760 J was used. As a result of the optimum distribution of Q as shown in the inset of figure 7(b), the calculated $T'(t)$ can reproduce the

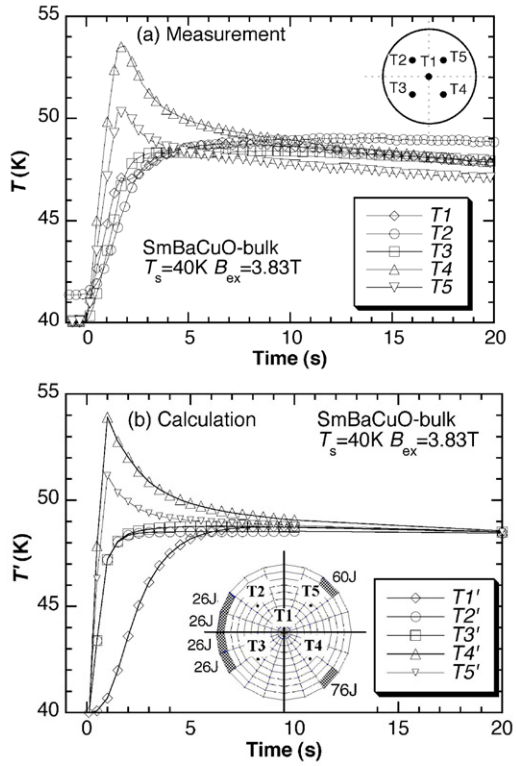

Figure 6. The time evolutions of (a) the measured temperatures $T(t)$ and (b) the calculated ones $T'(t)$ on the SmBaCuO bulk surface after applying a pulse field of $B_{ex} = 3.83$ T. The spatial distribution of the generated heat is also shown in the inset of (b).

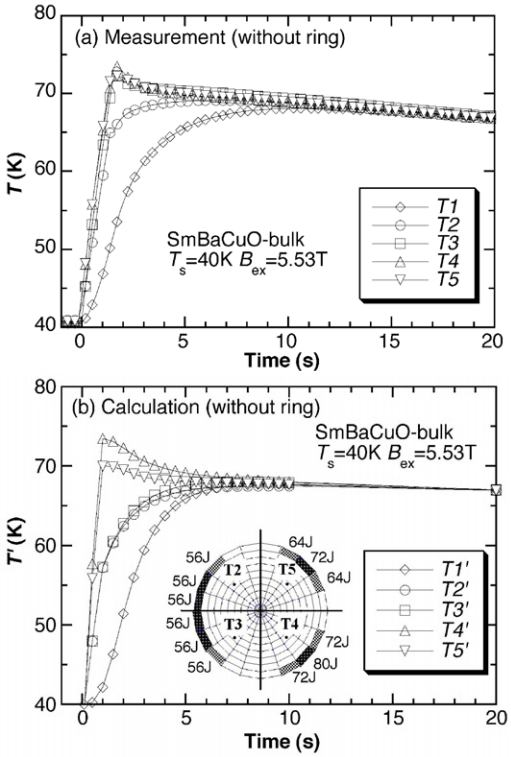

Figure 7. The time evolutions of (a) the measured temperature $T(t)$ and (b) the calculated ones $T'(t)$ on the surface of the SmBaCuO bulk after applying a pulse field of $B_{ex} = 5.53$ T. The spatial distribution of the generated heat is also shown in the inset of (b).

measured $T(t)$ at each position well. The slight difference between the calculated $T'(t)$ and the measured $T(t)$ may result from our assumption for the Q distribution; the heat source exists only in the outermost periphery element layer.

3.4. Effect of stainless steel ring setting

In our previous paper, we investigated the effect of setting a metal ring on the SmBaCuO bulk disc on the trapped field and the temperature rise during PFM [10, 11]. It was found that the total trapped flux Φ_T^P and the trapped field B_T^P were enhanced about 10–20% by setting a stainless steel (SUS) ring. A part of the heat generated in the peripheral region promptly transfers to the SUS ring. Figure 8(a) shows the time dependences of the measured temperature $T(t)$ of the SmBaCuO bulk with SUS ring after applying a pulse field of $B_{ex} = 5.53$ T at $T_s = 40$ K. An SUS ring 4 mm in thickness and 15 mm in height was tightly fixed onto the bulk disc using APIEZON-N grease. The temperature $T_{ring}(t)$ on the SUS ring was also monitored. It should be noticed that the $T(t)$ of $T1$–$T5$ increase, have a maximum similar to those for the same bulk without SUS ring, as shown in figure 7(a), and then decrease. $T_{ring}(t)$ gradually increases by about a half of $T1$–$T5$ and has a maximum at 15 s. The heat generation in the SUS ring due to the eddy current loss was confirmed to hardly take place because of the higher electrical resistivity. These results mean that a part of the generated heat Q in the bulk promptly transfers to the SUS ring. Figure 8(b) shows the calculated temperatures $T'(t)$ on the SmBaCuO bulk with SUS ring after applying a pulse field of $B_{ex} = 5.53$ T. In the calculation of $T'(t)$, the thermal conductivity κ (=5.5 W m^{-1} K^{-1}), the density d (=7.8 g cm^{-3}) and the specific heat C (=48.7 J kg^{-1} K^{-1}) of the stainless steel were used. The thermal contact resistance R_c(ring) between the bulk and the SUS ring was decided to be $1000/\kappa_{ab}$. The calculated $T'(t)$ at each position shown in figure 8(b) can roughly reproduce the measured $T(t)$ shown in figure 8(a). In this experimental setup, the SUS ring acts as a heat reservoir with a large heat capacity and a part of the generated heat in the bulk quickly transfers to the ring. Since the heat generation takes place under an adiabatic condition during PFM, the enhancement of the total heat capacity by attaching a heat reservoir with a large mass to the bulk is one of the possible techniques to reduce the temperature rise and then to enhance the trapped field B_T in the bulk.

4. Summary

The three-dimensional temperature profiles $T'(t, \vec{x})$ in the superconducting bulk disc after applying the pulse field have been calculated by the use of a finite element method (FEM). The calculated $T'(t, \vec{x})$ well reproduced the experimentally obtained $T(t, \vec{x})$ by distributing the generated heat Q appropriately in the periphery region of the bulk disc. From the analysis, the heat generation takes place in the bulk under adiabatic conditions during PFM and the Q values are about one or two orders of magnitude larger than the cooling power

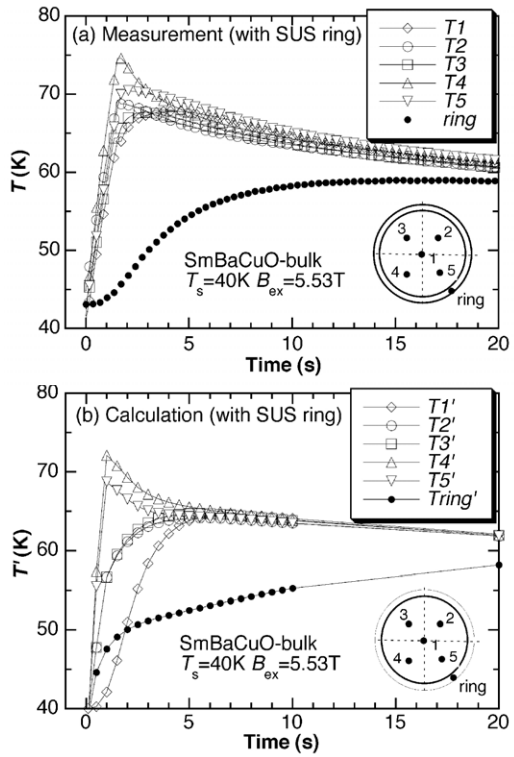

Figure 8. The time evolutions of (a) the measured temperature $T(t)$ and (b) the calculated ones $T'(t)$ of the SmBaCuO bulk with a stainless steel (SUS) ring after applying a pulse field of $B_{ex} = 5.53$ T.

of the GM cycle helium refrigerator used. These results suggest that the large heat generation is an indispensable issue and that it cannot be absorbed by the helium refrigerator promptly. In order to reduce the temperature rise during PFM, the dispersion of the generated heat to a metal ring set onto the bulk is one of the possible methods from the viewpoint of the heat propagation analysis.

Acknowledgments

This work is supported in part by a Grant-in-Aid for Scientific Research from the Ministry of the Education, Culture, Sports, Science and Technology, Japan (No. 17560001) and from Iwate Prefecture, Japan.

References

[1] Mizutani U, Hazama H, Matsuda T, Yanagi Y, Itoh Y, Sakurai K and Imai A 2003 *Supercond. Sci. Technol.* **16** 1207
[2] Fujishiro H, Oka T, Yokoyama K and Noto K 2003 *Supercond. Sci. Technol.* **16** 809
[3] Fujishiro H, Kaneyama M, Yokoyama K, Oka T and Noto K 2005 *Japan. J. Appl. Phys.* **44** 4919
[4] Fujishiro H, Yokoyama K, Oka T and Noto K 2004 *Supercond. Sci. Technol.* **17** 51
[5] Fujishiro H, Tateiwa T, Fujiwara A, Oka T and Hayashi H 2006 *Physica* C at press
[6] Ohsaki H, Shimosaki T and Nozawa N 2002 *Supercond. Sci. Technol.* **15** 754
[7] Fujishiro H, Yokoyama K, Kaneyama M, Oka T and Noto K 2004 *Physica* C **412–414** 646
[8] Fujishiro H and Kohayashi S 2002 *IEEE Trans. Appl. Supercond.* **12** 1124
[9] see http://ikebehp.mat.iwate-u.ac.jp/database.html
[10] Fujishiro H, Yokoyama K, Kaneyama M, Ikebe M, Oka T and Noto K 2005 *Physica* C **426–431** 594
[11] Fujishiro H, Yokoyama K, Kaneyama M, Oka T and Noto K 2005 *IEEE Trans. Appl. Supercond.* **15** 3762